IEEE Photonics Journal
An IEEE Photonics Society Publication

Open Access

Realization of Cascaded Frequency Conversions Using a Single $Gd_xY_{1-x}COB$ Crystal

Volume 8, Number 6, December 2016

Hongwei Qi
Zhengping Wang
Fapeng Yu
Xinguang Xu
Xian Zhao

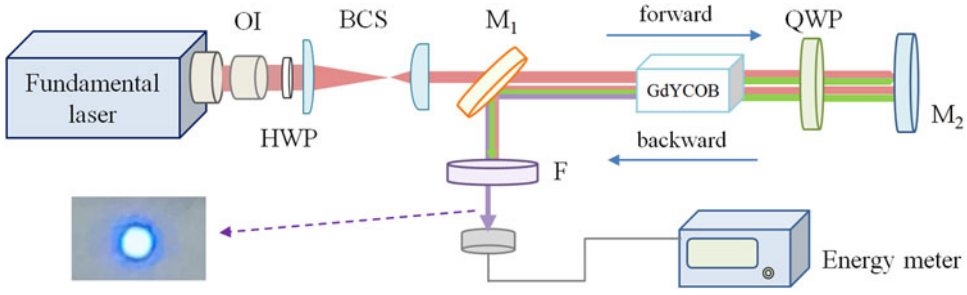

DOI: 10.1109/JPHOT.2016.2619069
1943-0655 © 2016 IEEE

IEEE photonics SOCIETY

IEEE

Realization of Cascaded Frequency Conversions Using a Single $Gd_xY_{1-x}COB$ Crystal

Hongwei Qi,[1,2] Zhengping Wang,[1,2] Fapeng Yu,[1,2] Xinguang Xu, and Xian Zhao[1,2]

[1]State Key Laboratory of Crystal Materials, Shandong University, Jinan 250100, China
[2]Key Laboratory of Functional Crystal Materials and Device (Shandong University), Ministry of Education, Jinan 250100, China

DOI:10.1109/JPHOT.2016.2619069

Manuscript received September 24, 2016; revised October 14, 2016; accepted October 15, 2016. Date of publication October 19, 2016; date of current version November 2, 2016. This work was supported in part by the National Natural Science Foundation of China under Grant 61178060, Grant 51202129, and Grant 91022034; in part by the Independent Innovation Foundation of Shandong University (2011GN056); and in part by the Natural Science Foundation for Distinguished Young Scholar of Shandong Province (2012JQ18). Corresponding authors: Z. Wang and F. Yu (e-mail: zpwang@sdu.edu.cn; fapengyu@sdu.edu.cn).

Abstract: In the field of nonlinear optics, cascaded frequency conversion is an effective method to obtain a solid-state laser source in the short wavelength region. By far, the most famous and popular frequency conversion approach is cascaded third-harmonic-generation (THG), which is composed of two steps: a phase-matching (PM) second-harmonic-generation, followed by a PM sum-frequency-generation. Correspondingly, two nonlinear optical (NLO) crystals are required. Theoretically, THG could be realized by utilizing only one crystal, as long as the frequency conversion processes occur at similar PM orientations and the polarization matching problem is solved. In this paper, we realized this approach by using one $Gd_xY_{1-x}COB$ crystal; an ultrawide angular acceptance was observed because the SHG process was noncritical phase matching, thereby providing the advantages of large angular acceptance and freedom from beam walk-off as the optimum PM approach in the NLO domain. Compared to the traditional cascaded THG configuration that requires two crystals, this configuration possesses the advantages of small volume, compactness, and low cost, all of which are favorable for practical applications.

Index Terms: Third-harmonic-generation, nonlinear optics, $Gd_xY_{1-x}COB$ crystal, ultraviolet laser.

1. Introduction

Currently, ultraviolet (UV) laser sources have been in great demand for various applications in a variety of fields, including material processing, laser chemistry, optical carving, rapid prototyping, laser printing, and spectroscopy [1], [2]. Several methods have been reported to obtain coherent light in this region [3]–[10]. Among these methods, the common approach is harmonic generation via nonlinear optical (NLO) crystals. The direct third-harmonic-generation (THG) based on third-order nonlinearity in a single crystal has been reported [3], but it is inefficient because of the low third-order optical nonlinearity. The quasi-phase-matched THG from a quasi-periodic optical superlattice (QPOS) in one crystal has also been demonstrated [5]; however, the QPOS technique is plagued

by some practical problems, such as complicated preparation processes and high price. As a result, currently, the most popular method is cascaded THG [6], which has many advantages including high efficiency, high energy, high stability, and good beam quality. Cascaded THG consists of two steps: a phase-matching (PM) second-harmonic-generation (SHG), followed by a PM sum-frequency-generation (SFG); correspondingly, two NLO crystals are required because of the different laser polarizations in SHG and SFG processes. However, in theory, cascaded THG could be realized by utilizing one crystal if the frequency conversion processes occur at similar PM orientations and if the polarization matching problem can be solved.

$Gd_xY_{1-x}Ca_4O(BO_3)_3$ ($Gd_xY_{1-x}COB$) is an excellent NLO crystal that has been extensively investigated [11]–[23]. These crystals possess many excellent properties, e.g., moderate NLO coefficients, large phase-matching range, high laser damage threshold, non-hygroscopicity, and stable physical, chemical and mechanical performance. As congruent melting compounds, these crystals can be grown to large sizes with high optical quality using the conventional Czochralski (Cz) pulling method.

In this paper, we realized cascaded THG in one $Gd_xY_{1-x}COB$ crystal by introducing a quarter-wave plate (QWP) and a total reflection mirror to solve the laser polarization matching problem. The QWP was used to adjust the polarization of the SHG wave, and the total reflection mirror was used to form a round-trip optical path to realize the SHG and SFG processes in the $Gd_xY_{1-x}COB$ crystal successively. The theoretical design and characteristics of the scheme were described in detail, and cascaded THG outputs of 1064 nm and 1053 nm lasers were demonstrated with ultra-wide angular acceptance because the relevant SHG processes were non-critical phase-matching (NCPM) processes. In addition to the advantages of NCPM, this configuration can effectively reduce the production cost and the device sizes, representing a significant improvement over the traditional configuration.

2. Non-critical phase-matching of $Gd_xY_{1-x}COB$ crystal

For biaxial optical crystals, NCPM is the PM along the principal axes of the refractive index. As a special PM configuration, its angular acceptance is much larger than those of other PM configurations, and there is no beam walk-off. Thus, NCPM is also called the “Optimum PM”. In addition, NCPM usually possesses the advantage of high utilization of the as-grown crystal. It has been reported that NCPM can be realized in LiB_3O_5 by utilizing its special refractive index temperature characteristic. In fact, NCPM can also be realized in $Gd_xY_{1-x}COB$ mixed crystals by changing the compositional parameter x to control the optical birefringence [23]–[27]. Our previous studies have revealed that the NCPM type-II SHG and type-I THG of 1064 nm and 1053 nm lasers can be realized along the Y-axis by adjusting the compositional parameter x [27], [28]. The dependences of NCPM wavelength on the compositional parameter x were linearly fitted according to the experimental data at room temperature, as shown in Fig. 1.

The corresponding values can be calculated using the fitting formulas [28]:

$$\begin{cases} SHG : y = 1024 + 224x \\ THG : y = 1025 + 202x \end{cases} \tag{1}$$

where y is the NCPM wavelength, and x is the compositional parameter of the Gd ions.

The compositional parameter x for SHG are determined to be ~ 0.129 for 1053 nm and ~ 0.178 for 1064 nm, and the corresponding values for THG are ~ 0.139 and ~ 0.193, respectively. The NCPM SHG and THG compositions are very similar, indicating that the SHG and THG components can be processed along the same direction (i.e., Y-axis) within a specific composition range. Nevertheless, prior to this work, two crystal blocks were required to realize the final THG output because the 2ω polarization generated by the type-II SHG lies along the X-axis of the crystal, whereas the polarization of 2ω wave is required to be along the Z-axis of the crystal for type-I SFG.

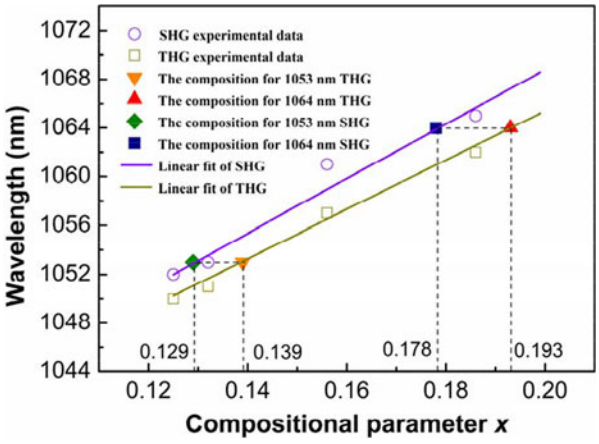

Fig. 1. Dependence of the NCPM wavelength on the compositional parameter x at room temperature.

3. The theoretical design and the experimental configuration

3.1. The theoretical design

In theory, if the polarization matching problem is solved, then cascaded THG in one $Gd_xY_{1-x}COB$ crystal could be realized. To solve this problem, we proposed a solution based on the polarization rotation characteristics of the wave plate. In this design, a QWP is used to control the laser polarizations, and a total reflection mirror M_2 is used to form a round-trip optical path. The key is that the linear polarization of the fundamental wave, the bisection plane of the Z-axis and X-axis of the $Gd_xY_{1-x}COB$ crystal and the optical axis of the QWP should be consistent. In this manner, the QWP will not change the ω polarization during the whole process, whereas the polarization of 2ω wave generated by type-II SHG on the X-axis will be rotated 90° to the Z-axis after the forward and backward passing through the QWP twice, as can be explained by the Jones matrix.

The Jones matrices of the 2ω wave polarization after type-II SHG, the QWP and the total reflection mirror M_2 can be expressed as

$$J_{E_x} = \begin{bmatrix} 1 \\ 0 \end{bmatrix}$$
$$J_{\lambda/4} = \begin{bmatrix} \cos^2\theta + i\sin^2\theta & \cos\theta\sin\theta(1-i) \\ \cos\theta\sin\theta(1-i) & i\cos^2\theta + \sin^2\theta \end{bmatrix} \quad (2)$$
$$J_{M_2} = \begin{bmatrix} 1 & 0 \\ 0 & -1 \end{bmatrix}$$

where θ is the angle between the fast-axis of the QWP and the X-axis of the crystal. In the forward optical path, $\theta = 45°$, and in the backward optical path, $\theta = -45°$; thus, the Jones matrices of the QWP can be transformed into the following forms:

$$J_{\lambda/4} = \frac{1}{2}\begin{bmatrix} 1+i & 1-i \\ 1-i & i+1 \end{bmatrix} J'_{\lambda/4} = \frac{1}{2}\begin{bmatrix} 1+i & i-1 \\ i-1 & i+1 \end{bmatrix} \quad (3)$$

When the 2ω wave passes through the QWP for the first time, it will become a circularly polarized wave E'_x, as given by the Jones matrix:

$$E'_x = \frac{1}{2}\begin{bmatrix} 1+i & 1-i \\ 1-i & i+i \end{bmatrix}\begin{bmatrix} 1 \\ 0 \end{bmatrix} = \frac{1}{2}\begin{bmatrix} 1+i \\ 1-i \end{bmatrix}$$

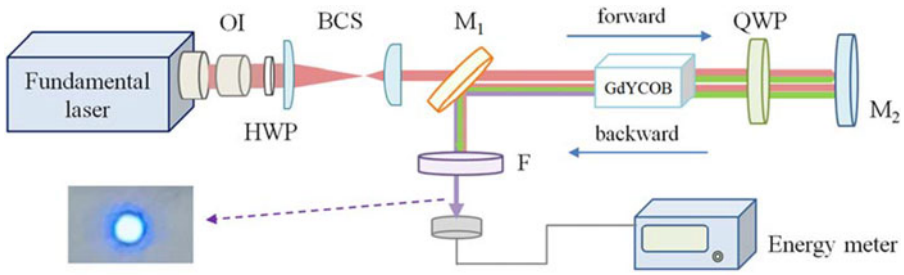

Fig. 2. Experimental setup for the cascaded THG.

After the reflection of the M_2, the circularly polarized 2ω wave becomes E''_x:

$$E''_x = \frac{1}{2}\begin{bmatrix} 1 & 0 \\ 0 & -1 \end{bmatrix}\begin{bmatrix} 1+i \\ 1-i \end{bmatrix} = \frac{1}{2}\begin{bmatrix} 1+i \\ i-1 \end{bmatrix}$$

Next, after it passes through the QWP for the second time, the 2ω wave is rotated 90° to become E_z:

$$E'''_x = \frac{1}{2}\begin{bmatrix} 1+i & i-1 \\ i-1 & i+1 \end{bmatrix}\frac{1}{2}\begin{bmatrix} 1+i \\ i-1 \end{bmatrix} = \frac{1}{4}\begin{bmatrix} 0 \\ -4 \end{bmatrix} = \begin{bmatrix} 0 \\ -1 \end{bmatrix} = E_z.$$

The result is that the required polarization condition of the 2ω wave for the type-I SFG is fulfilled. Next, in the process of back propagation, the Z-polarized 2ω wave can interact with the Z-polarized component of the residual ω wave in the $Gd_xY_{1-x}COB$ crystal to achieve type-I SFG. As a result, the THG output can be obtained with only one $Gd_xY_{1-x}COB$ crystal.

3.2. The experimental configuration

In the experiments, we prepared two $Gd_xY_{1-x}COB$ crystals, which have the compositions for NCPM type-II SHG of 1064 nm ($x = 0.178$) and 1053 nm ($x = 0.129$), respectively. These crystals were oriented along their refractive index principal axes (X, Y and Z) and cut along the Y-axis (which is the PM direction for NCPM SHG and SFG) with dimensions of 10 mm × 10 mm × 5 mm. Their transmission surfaces were polished but uncoated.

The experimental setup is exhibited in Fig. 2. For the output of a 355 nm laser, a mode-locked Nd:YAG laser was employed as the fundamental light source with a wavelength of 1064 nm, a pulse width of 40 ps, a beam diameter of 8 mm, and a repetition rate of 10 Hz. The output of the fundamental laser was a vertical linearly polarized beam, and a 1064 nm half-wave plate (HWP) was used to adjust its linear polarization. An optical isolator (OI) was used to avoid the disturbance of the returned beams going into the fundamental light source. To increase the energy density of the fundamental laser, a beam compression system (BCS), which was composed of two plane-convex lens ($f = 200$ mm and 50 mm, respectively), was used. The original 8 mm diameter of the fundamental beam was reduced to 2 mm. A beam splitter M_1 with high transmittance for the fundamental wave (T = 90% @ 1064 nm) and high reflection for the 2ω and 3ω waves (R > 99% @ 532 nm and 355 nm) was placed at a 45° inclination angle to the main light path. The crystal block ($x = 0.178$) was placed in a copper cube, whose temperature was controlled with an accuracy of ± 0.1 °C. The copper cube was sealed to prevent thermal diffusion, and its incident and output faces were covered with pieces of quartz glass to permit high transmittance from the UV to the near infrared. The temperature-controlling device was fixed on a motor driven rotation stage with a high precision of 0.00125°. A 532 nm mica QWP was inserted between the $Gd_xY_{1-x}COB$ crystal block and the total reflection mirror M_2. The optical axis of the QWP was parallel to the polarization of the fundamental wave and the bisection plane of Z-axis and X-axis of the crystal. M_2 was a total

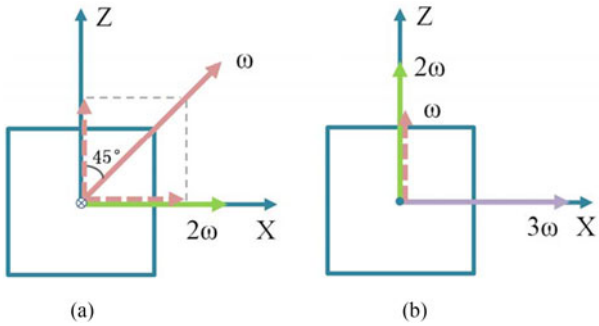

Fig. 3. (a) Polarization compositions of the type-II SHG process ($Z_\omega + X_\omega \rightarrow X_{2\omega}$) in the forward optical path. (b) Polarization compositions of the type-I SFG process ($Z_{2\omega} + Z_\omega \rightarrow X_{3\omega}$) in the backward optical path.

reflection mirror at 1064 nm and 532 nm that was used for reflecting the fundamental and 2ω waves to ensure the beams return to the QWP and the crystal for SFG. After the reflection of M_1, the 3ω laser beam was selected out from the unconverted fundamental and 2ω lasers by the filter F ($T = 48.5\%$ at 355 nm, $T < 0.5\%$ at 1064 nm and 532 nm). Next, the THG output energy was measured by an energy meter. The polarization compositions of the type-II SHG process ($Z_\omega + X_\omega \rightarrow X_{2\omega}$) in the forward optical path are shown in Fig. 3(a), and the polarization compositions of the type-I SFG process ($Z_{2\omega} + Z_\omega \rightarrow X_{3\omega}$) in the backward optical path are shown in Fig. 3(b).

Utilizing another $Gd_xY_{1-x}COB$ crystal sample with the composition $x = 0.129$, cascaded THG experiments of 1053 nm were also conducted. The experimental configuration was similar to the setup mentioned above. A Nd:YLF laser was employed as the fundamental light source. The output of the fundamental laser was a vertical linearly polarized beam with a wavelength of 1053 nm, a beam diameter of 7 mm, a pulse width of 1 ns, and a repetition rate of 1 Hz. Its polarization was adjusted using a 1053 nm HWP. In addition, a 526 nm mica QWP was utilized.

4. Results and discussion

The THG light appeared by adjusting the optical axis of the QWP to be parallel to the linear polarization of the fundamental wave, as well as the bisection plane of the Z-axis and X-axis of the $Gd_xY_{1-x}COB$ crystal. While tuning the inclined angle of M_2, THG light was always output within the scope of the adjustment; this capability was attributed to the characteristic of NCPM. When the QWP was removed, the THG light disappeared. When the wave plate was rotated, the THG output intensity changed periodically. These phenomena verified the theoretical design scheme discussed previously.

Next, after removing the QWP and M_2 in Fig. 2, the SHG conversion efficiencies were measured. A filter with $T < 0.5\%$ at 1064 nm and 1053 nm and $T = 81\%$ at 532 nm and 526 nm was placed to the right of the $Gd_xY_{1-x}COB$ crystal to block the fundamental laser, and the transmitted SHG wave was detected by an energy meter. At an ambient temperature of 24 °C, NCPM SHG was realized; the maximum SHG conversion efficiency was 15% at a fundamental energy of 1.8 mJ for the 1064 nm laser and 13% at a fundamental energy of 13 mJ for the 1053 nm laser. Both the conversion efficiencies were saturated when the fundamental energies were increased. The relatively low efficiency originated from the small effective NLO coefficient ($d_{\text{eff}} = d_{31} \asymp -0.3\,\text{pm/V}$ [14]) for this PM style in the $Gd_xY_{1-x}COB$ crystal and the short sample length (5 mm).

Although the crystal ($x = 0.178$) realized NCPM SHG of 1064 nm along the Y-axis at 24 °C, the SFG PM directions deviated from the Y-axis for an exterior angle of approximately 10° (i.e., an internal angle of $\sim 5.9°$) that were observed by adjusting the inclined angle of M_2. As a result, two strong directions of UV laser output were observed: the SFG PM directions that are symmetrically distributed on both sides of the Y-axis. Considering the transmittance of F and the fundamental

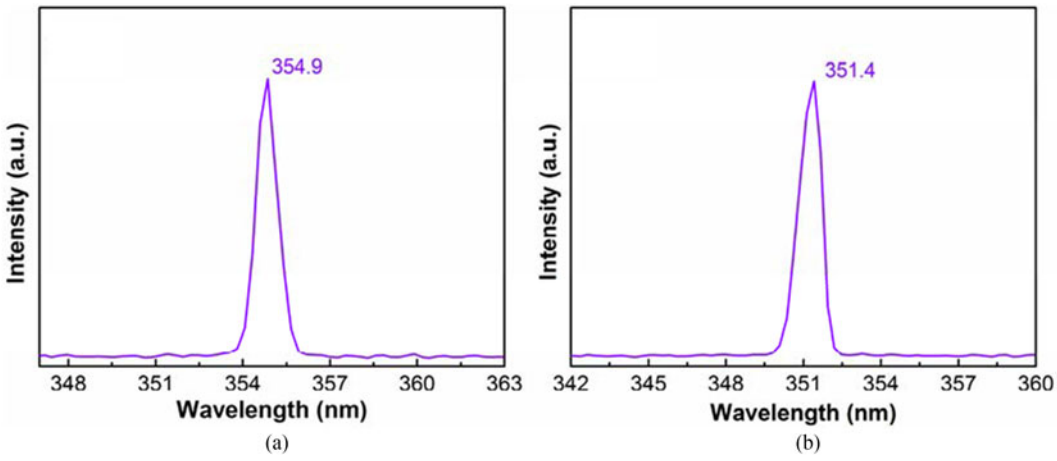

Fig. 4. The 3ω output spectra of (a) the 1064 nm laser and (b) the 1053 nm laser.

Fresnel loss of the $Gd_xY_{1-x}COB$ crystal, the maximum 3ω energy of 0.05 mJ was obtained for the 2.2 mJ fundamental laser, corresponding to an overall conversion efficiency of 2.3%. Considering the SHG energy was $\sim$ 0.33 mJ, the optical conversion efficiency from 2ω to 3ω was 15.2%. With a spectrum analyzer, the central wavelength of the THG output was measured to be 354.9 nm, as shown in Fig. 4(a).

According to the refractive index temperature characteristic of the $Gd_xY_{1-x}COB$ crystal, by elevating the crystal temperature, the SFG PM angles changes toward the Y-axis, i.e., the NCPM direction of θ, $\phi() = (90^\circ, 90^\circ)$. In our experiments, when the crystal temperature was increased to 145 °C, the NCPM SFG was realized, and only one strong direction of UV laser output was observed i.e., along the Y-axis. However, during the whole process of heating, the SHG conversion efficiency gradually reduced because the variation of crystal refractive index caused increasing deviations from the optimum NCPM SHG situation. Because the SHG process was the basis of the SFG process, the SFG conversion efficiency did not present an obvious improvement when the NCPM SFG condition was reached.

For the cascaded THG experiments of the 1053 nm laser, similar results were obtained with the $Gd_xY_{1-x}COB$ crystal ($x = 0.129$). The maximum THG output energy was 0.3 mJ at a fundamental energy of 16.6 mJ. The overall conversion efficiency was 1.8%, and the corresponding optical conversion efficiency from SHG to SFG was 13.8%. The corresponding THG output spectrum is shown in Fig. 4(b).

5. Conclusions

In this paper, cascaded THG utilizing one $Gd_xY_{1-x}COB$ crystal was realized using a specially designed configuration. A QWP was used to adjust the polarization of the SHG wave, and a round-trip optical path was used to realize the SHG and SFG processes, successively. The THG outputs possessed ultra-wide angular acceptance because the SHG processes were NCPM, i.e., along the Y-axis of the $Gd_xY_{1-x}COB$ crystal. Although the present optical conversion efficiency is not very high, it is expected to be greatly improved in the future by utilizing a longer crystal sample because the NCPM style possesses the advantages of large angular acceptance and no beam walk-off, and its action length is infinite in theory. In summary, this special configuration is easy to adjust and effectively reduces the production cost and the device sizes, which are favorable features for practical application. Moreover, this approach can be extended to other NLO materials, as long as the required cascaded frequency conversion processes occur under similar crystal orientations.

This technique enriches the design concepts of NLO components, and it is anticipated to be applied in practice in the near future.

References

[1] P. A. Norreys *et al.*, "Efficient extreme UV harmonics generated from picosecond laser pulse interactions with solid targets," *Phys. Rev. Lett.*, vol. 76, no. 11, Mar. 1996, Art. no. 1832.

[2] R. J. Gray *et al.*, "Surface transport of energetic electrons in intense picosecond laser-foil interactions," *Appl. Phys. Lett.*, vol. 99, no. 17, Oct. 2011, Art. no. 171502.

[3] K. Miyata, V. Petrov, and F. Noack, "High-efficiency single-crystal third-harmonic-generation in BiB_3O_6," *Opt. Lett.*, vol. 36, no. 18, pp. 3627–3629, Sep. 2011.

[4] S. N. Zhu, Y. Y. Zhu, and N. B. Ming, "Quasi-phase-matched third-harmonic generation in a quasi-periodic optical superlattice," *Science*, vol. 278, no. 5339, pp. 843–846, Oct. 1997.

[5] A. S. Aleksandrovsky, A. M. Vyunishev, A. I. Zaitsev, and V. V. Slabko, "Random quasi-phase-matched nonlinear optical conversion of supercontinuum to the ultraviolet," *Appl. Phys. Lett.*, vol. 103, no. 25, Dec. 2013, Art. no. 251104.

[6] X. Ya, Q. Liu, M. Gong, X. Fu, and D. Wang, "High-repetition-rate high-beam-quality 43 W ultraviolet laser with extra-cavity third harmonic generation," *Appl. Phys. B*, vol. 95, no. 2, pp. 323–328, May 2009.

[7] D. Coquillat *et al.*, "Enhanced second-and third-harmonic generation and induced photoluminescence in a two-dimensional GaN photonic crystal," *Appl. Phys. Lett.*, vol. 87, no. 10, Sep. 2005, Art. no. 101106.

[8] N. Morita, L. H. Lin, and T. Yajima, "Generation of picosecond UV pulses by stimulated anti-Stokes Raman scattering," *Appl. Phys. B*, vol. 31, no. 2, pp. 63–67, Jun. 1983.

[9] S. Suntsov, D. Abdollahpour, D. G. Papazoglou, and S. Tzortzakis, "Filamentation-induced third-harmonic generation in air via plasma-enhanced third-order susceptibility," *Phys. Rev. A*, vol. 81, no. 3, Mar. 2010, Art. no. 033817.

[10] V. Grubsky and J. Feinberg, "Phase-matched third-harmonic UV generation using low-order modes in a glass micro-fiber," *Opt. Commun.*, vol. 274, no. 2, pp. 447–450, Jun. 2007.

[11] G. Aka *et al.*, "Linear- and nonlinear-optical properties of a special gadolinium calcium oxoborate crystal, $Ca_4GdO(BO_3)_3$," *J. Opt. Soc. Amer. B*, vol. 14, no. 9, pp. 2238–2247, Sep. 1997.

[12] M. Iwai, T. Kobayashi, H. Furuya, Y. Mori, and T. Sasaki, "Crystal growth and optical characterization of rare-earth (Re) calcium oxyborate $ReCa_4(BO_3)_3$ (Re=Y or Gd) as special nonlinear optical material," *Jpn. J. Appl. Phys.*, vol. 36, no. 2, pp. L276–L279, Mar. 1997.

[13] M. V. Pack *et al.*, "Measurement of the $\chi^{(2)}$ tensor of $GdCa_4O(BO_3)_3$ and $YCa_4O(BO_3)_3$ crystals," *J. Opt. Soc. Amer. B*, vol. 22, no. 2, pp. 417–425, Feb. 2005.

[14] Z. P. Wang *et al.*, "The second-harmonic-generation property of $GdCa_4O(BO_3)_3$ crystal with various phase-matching directions," *Opt. Commun.*, vol. 187, no. 4, pp. 401–405, Jan. 2001.

[15] Y. T. Fei *et al.*, "Large-aperture YCOB crystal growth for frequency conversion in the high average power laser system," *J. Cryst. Growth*, vol. 290, no. 1, pp. 301–306, Apr. 2006.

[16] Y. Q. Liu *et al.*, "Type-II second-harmonic-generation properties of YCOB and GdCOB single crystals," *Opt Exp.*, vol. 23, no. 3, pp. 2163–2173, Feb. 2015.

[17] H. Furuya *et al.*, "Dependence of gray-track threshold of GdYCOB on the crystal growth atmosphere," *J. Cryst. Growth*, vol. 229, no. 1, pp. 265–269, Jul. 2001.

[18] G. Aka *et al.*, "Overview of the laser and non-linear optical properties of calcium-gadolinium-oxo-borate $Ca_4GdO(BO_3)_3$," *J. Alloys Compounds*, vol. 303, pp. 401–408, May 2000.

[19] L. H. Yu *et al.*, "Experimental demonstration of joule-level non-collinear optical parametric chirped-pulse amplification in yttrium calcium oxyborate," *Opt. Lett.*, vol. 37, no. 10, pp. 1712–1714, May 2012.

[20] I. V. Kityk and A. Mefleh, "Electronic structure and optical response in $Ca_4GdO(BO_3)_3$ single crystals," *Physica B*, vol. 262, pp. 170–176, Feb. 1999.

[21] N. Umemura *et al.*, "90° phase-matching properties of $YCa_4O(BO_3)_3$ and $Gd_xY_{1-x}Ca_4O(BO_3)_3$," *Jpn. J. Appl. Phys.*, vol. 40, no. 1, pp. 596–600, Feb. 2001.

[22] N. Umemura *et al.*, "Temperature phase-matching properties for harmonic generation in $GdCa_4O(BO_3)_3$ and $Gd_xY_{1-x}Ca_4O(BO_3)_3$," *Appl. Opt.*, vol. 45, no. 16, pp. 3859–3863, Jun. 2006.

[23] H. Furuya *et al.*, "Crystal growth and characterization of $Gd_xY_{1-x}Ca_4O(BO_3)_3$ crystal," *J. Cryst. Growth*, vol. 198, pp. 560–563, May 1999.

[24] A. Zoubir *et al.*, "Non-critical phase-matched second harmonic generation in $Gd_xY_{1-x}COB$," *Appl. Phys. B*, vol. 77, no. 4, pp. 437–440, Oct. 2003.

[25] P. Burmeste *et al.*, "Type-I non-critically phase-matched second-harmonic generation in $Gd_{1-x}Y_xCa_4O(BO_3)_3$," *Appl. Phys. B*, vol. 68, no. 6, pp. 1143–1146, Jun. 1999.

[26] M. Yoshimura *et al.*, "Noncritically phase-matched frequency conversion in $Gd_xY_{1--x}Ca_4O(BO_3)_3$ crystal," *Opt. Lett.*, vol. 68, no. 4, pp. 193–195, Feb. 1999.

[27] Z. P. Wang *et al.*, "Non-critical phase matching of $Gd_xY_{1-x}Ca_4O(BO_3)_3$ ($Gd_xY_{1-x}COB$) crystal," *Solid State Commun.*, vol. 120, no. 9, pp. 397–400, Nov. 2001.

[28] H. W. Qi *et al.*, "Non-critical phase-matched second-harmonic-generation and third-harmonic-generation of 1053 nm lasers in $Gd_xY_{1-x}COB$ crystal," *Opt. Mater. Exp.*, vol. 6, no. 5, pp. 1576–1586, May 2016.